Cold Regions Science and Technology 111 (2015) 80–94

Contents lists available at ScienceDirect

Cold Regions Science and Technology

journal homepage: www.elsevier.com/locate/coldregions

# A deep insight into avalanche transceivers for optimizing rescue

N. Ayuso *, J.A. Cuchí, F. Lera, J.L. Villarroel

*Aragón Institute of Engineering Research (I3A), I+D+i Building, Mariano Esquillor s/n, 50018 Zaragoza, Spain*
*Group of Technologies in Hostile Environments (GTE) University of Zaragoza, 50018 Zaragoza,Spain*

ARTICLE INFO

*Article history:*
Received 25 October 2013
Received in revised form 9 December 2014
Accepted 10 December 2014
Available online 16 December 2014

*Keywords:*
Avalanche rescue
Avalanche transceiver
Numerical simulation
Field tests

ABSTRACT

It is well known that in order to increase the chances of survival after an avalanche accident, the rescue time has to be minimized. Therefore, the accurate and prompt location of an avalanche victim is of vital importance. Nowadays, searching with avalanche transceivers is the only reliable method for locating a completely buried victim immediately after an accident. The present work is firstly focused on the magnetic field pattern generated by an avalanche transceiver and how it is perceived depending on the number of receiving antennas. The influence of the snow and soil media is theoretically studied. The computations show that the magnetic field is notably distorted by the soil at distances from the transmitter that can take place during the signal and coarse search. The location of the victim is usually directly inferred from the maximum signal position. However, the computations clearly show that this can be wrong. There is a location error limited to 50% of the burial depth for one and two-antenna receivers whereas for three-antenna transceivers, assuming location takes place within the third antenna range, this figure is reduced to 25% of the burial depth. Furthermore, real tests show that the cross-like search method using three-antenna receivers can be inefficient depending on the algorithm used for the distance calculation for burial depths greater than 1.5 m. As a result, a new search technique, called the bisector method, is proposed and experimentally validated. In addition, a new transmission mode mainly directed to minimize the location error is suggested. This is a vertical transmission that can optimize the search. The present theoretical and experimental outcomes will contribute to further progress in rescue operations conducted with avalanche transceivers.



## 1. Introduction

Snow avalanches claim scores of victims every year in mountainous areas, among local population, mountaineers, pilgrims, transportation and electrical power workers, military personnel and sportsmen.

It is not easy to obtain reliable figures but a good estimation may be an average of 200 people killed by avalanches every year. Working with data relating to sports men and women affected by avalanches in developed countries, Etter et al. (2004) estimated a total of 1593 deaths, during the period 1983/84 to 1992/93 and 1599 deaths in the following decade. Despite an increasing number of participants in outdoor winter sports, victim statistics remain stable with important temporary variations mainly due to local adverse snow and weather conditions (Jomelli et al., 2007).

International data are regularly presented in IKAR-CISA[1] reports, the best aggregated information on the issue. However, information on some countries, such as Spain, is not complete. Table 1 shows statistics according to the type of activity practiced by avalanche victims. In North America, avalanches are taking a growing toll on back-country skiers and snow-mobile users. In Europe, the highest rates of victims are back-country skiers followed by free ride-skiers and mountaineers. On the other hand, there is also a general downward trend of victims in controlled areas such as within the boundaries of ski resorts.

A number of papers published in several technical journals, usually preceded as communications in the Proceedings of the International Snow Science Workshop, present more detailed information on avalanche victims in given areas, usually in the Alpine arc or USA–Canada (e.g. Zweifel et al., 2012).

For obvious reasons, a significant number of these papers are devoted to the medical aspects of accidents (Brugger et al., 2001; Brugger et al., 2013; Falk et al., 1994; Haegeli et al., 2011). Burial time, burial depth and type of avalanche are important factors affecting the possibilities of recovering a victim alive. Burial time is the critical factor, as the probability of survival declines sharply after 8 min. Depth is also an important factor in rescue due to the increasing snow volume to be removed in addition to the difficulty of finding the victim. Data on the depth of burial of avalanche victims show only few cases of survivors buried at a depth of over 2 m (Tschirky et al., 2000).

Obviously, the victims of an avalanche must be rescued as soon as possible. The first people involved in the rescue are the companions of the buried subjects. Statistics presented by Slotta-Bachmayr (2005)

* Corresponding author at: Aragón Institute of Engineering Research (I3A), I+D+i Building, Mariano Esquillor s/n, 50018 Zaragoza, Spain.
*E-mail address:* nayuso@unizar.es (N. Ayuso).

[1] International Commission for Alpine Rescue.

http://dx.doi.org/10.1016/j.coldregions.2014.12.005

**Table 1**
Victims of snow avalanches according to activity (CISA-ICAR, 2010).

| 2*Season | Backcountry skiing | 2*Freeride | On skirun | 2*Alpinist | Snow-mobile | 2*Other |
|---|---|---|---|---|---|---|
| 2009/2010 | 93 | 37 | 2 | 39 | 24 | 17 |
| 2008/2009 | 69 | 44 | 3 | 19 | 38 | 23 |
| 2007/2008 | 68 | 25 | 3 | 24 | 24 | 12 |
| 2006/2007 | 60 | 21 | 0 | 21 | 11 | 7 |
| 2005/2006 | 77 | 59 | 2 | 18 | 14 | 22 |
| 2004/2005 | 95 | 41 | 2 | 25 | 7 | 14 |

show a significant survival decline if external rescue teams are involved due to the transportation time.

In addition to trained rescue dogs, the harmonic radar (RECCO) has been used by professional rescuers to locate buried victims. However, to date, avalanche rescue transceivers are the only technology that allows a fast and reliable search of completely buried victims by their companions (Genswein et al., 2009; Schweizer and Krüsi, 2003). The device can operate both as transmitter and receiver using solenoid antennas with ferrite cores as transceivers. For normal use, the avalanche transceiver generates a pulsed magnetic field of 457 kHz. Its specifications are regulated by the European standard *ETS 300718* (ETSI, 2001). If a victim is buried, another transceiver switched to the search mode can be used to detect and locate the signal of the victim's avalanche transceiver.

Many studies have demonstrated the usefulness of the device (Slotta-Bachmayr, 2005; Tschirky et al., 2000; Valt et al., 2009). Since the origin of avalanche rescue transceivers in the 1960s, a lot of work has been done by manufacturers resulting in yearly enhancements (e.g. digital transceivers, three antenna transceivers, multiple burial management, etc.). This work is normally protected by patents or more often by industrial secrecy, which can be considered a drawback for a faster development of this technology.

Associations such as CISA-IKAR, and single researchers have carried out the important task of testing and comparing the performance of commercial avalanche transceivers. Examples are works by Schweizer and Krüsi (2003) or Schreilechner et al. (2010). Some public research work has been done on avalanche transceiver technology. Michahelles et al. (2003) proposed to incorporate sensors to measure vital signs and environmental conditions to enhance avalanche transceiver search decisions. The processing of emitted signals has been studied in works such as Meier (2006) or Salós et al. (2007). In Matzner (2008) some functional aspects of modern transceivers were analyzed in order to design improvements.

Moreover, important work has been done on developing the best search strategies with standard avalanche transceivers. Currently, the basis of the search procedure is well established (searching for the first signal, following field flux lines and the final fine search). Researchers have attempted to bring greater depth to the classical method improving the search. For example, Genswein et al. (2009) proposed the optimization of the search strip width to minimize the search duration and Edgerly (2002) suggested a new fine search technique for solving deep burials. New search strategies based on the incorporation of a GPS receiver and new processing algorithms have also been proposed Piniés and Tardós (2006).

In contrast, there is a lack of studies concerning the core of the use of avalanche transceivers, that is the magnetic field generated by the transceiver and how it is perceived by the receiver. Lind and Smythe (1984) and Lind (1994) analyzed the avalanche transceiver performance taking into account the near field model and proposed some suggestion for modified use strategies. Ayuso et al. (2007) studied the distortions induced by the snow and the soil for any field component and source orientation.

The objective of this paper is to present the research undertaken by the Group of Technologies in hostile Environments (GTE) concerning this topic. We will show how the soil and the snow cover affect the field generated by the avalanche transceiver and its influence in the search phases. We also analyze how the magnetic field is perceived depending on the number of receiving antennas. The errors in positioning the victim will then be computed by the maximum signal offset. The theoretical work is supported by field tests. Finally, a new fine search method for modern digital transceivers with three antennas is proposed. In addition, a new transmission mode based on ensuring a vertical transmission is suggested. As a result, the search time and the localization error could be minimized. Consequently, a real increase in the survival chances of an avalanche victim could be achieved.

The paper is structured as follows. Section 2 reviews the fundamentals of the classical avalanche transceiver search. Section 3 studies theoretically the propagation of the magnetic field taking into account the effects of the snow cover and the soil for any orientation of the transmitter with respect to the air–snow–soil interfaces. Section 4 analyzes the location accuracy based on how the magnetic field is perceived by the avalanche transceiver. Corresponding field tests are presented in Section 5. Section 6 proposes different approaches for improving search

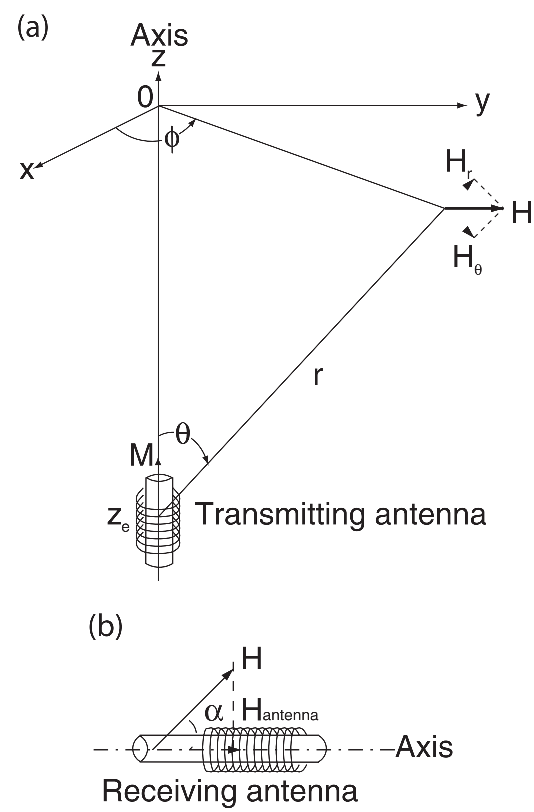


**Fig. 1.** (a): Magnetic dipole source and magnetic field components. (b): Sensed field ($H_{antenna}$) according to the relative orientation between the magnetic field and the axis of the receiving antenna.

by avalanche transceivers. Finally, the conclusions of the work are given in Section 7.

## 2. Basics of search by avalanche transceivers

### *2.1. Avalanche transceivers as magnetic dipole transmitters and receivers*

An avalanche transceiver transmitter drives a 457 kHz current through a wired ferrite core loop. Details are specified in the standard *ETS 300718* (ETSI, 2001). This results in a magnetic dipole that generates a magnetic moment $M$ according to the description shown in Fig. 1a

Traditionally, the surrounding media is considered a vacuum and the effects of the snow and underlying soil are discarded. Therefore, the near field limit is assumed as the transmitter-to-receiver range, $r$, satisfies the condition $r \ll \lambda_0/2\pi \approx 104$ m where $\lambda_0$ is the free-space wavelength. Consequently, the magnetic field intensity due to a magnetic dipole source centered at the origin and transmitting along the z-axis can be conveniently written in the spherical coordinate system as:

$$H_r = \frac{M}{2\pi r^3}\cos\theta \tag{1}$$

$$H_\theta = \frac{M}{4\pi r^3}\sin\theta \tag{2}$$

$$H_\phi = 0 \tag{3}$$

and the magnitude of the field as

$$H = \frac{M}{4\pi r^3}\sqrt{1+3\cos^2\theta}. \tag{4}$$

For a single antenna device, on reception the sensed magnetic field is determined by the relative orientation, $\alpha$, between the magnetic field and the axis of the receiving antenna (see Fig. 1b):

$$H_{antenna} = H \cdot \cos\alpha. \tag{5}$$

There are currently avalanche transceivers including one, two or three receiving antennas orthogonally placed in the case. Furthermore, the avalanche transceivers can operate with analog or digital technology. The former transforms the received field into audible tones or luminous indications of the intensity of the signal. The latter can display additional information to assist during the search, such as an estimation of the distance or the direction to approach the victim. The search operation described below is thus mainly conditioned by the number of antennas that the receiver has.

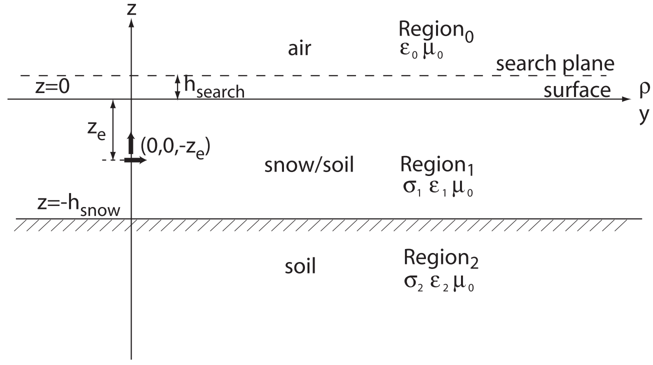


**Fig. 2.** Propagation models description.

**Table 2**
Simulation parameters set-up.

| Parameters | | Half-space | Three-layered |
|---|---|---|---|
| $h_{search}$ | Signal/coarse | 1.0 | 1.0 |
| | Fine | 0 | 0 |
| $z_e$ | | 1.0 | 1.0 |
| $h_{snow}$ | | – | 3.0 |

### *2.2. Stages of the search by avalanche transceivers*

The current search techniques for a single victim and a single rescuer are based on the simple geometry of the magnetic field described by Eqs. (1)–(3). Fundamentally, the search consists of the following three stages:

- *Signal search*. Searching for the first signal systematically prospecting the avalanche area by parallel lines. This phase comprises distances that are usually greater than 60 m from the transmitter. The search strip width is indicated by manufacturer and model but there are different methods for its optimal estimation (Schweizer, 2007), e.g. a width of 50 m for a transceiver with a maximum range of 60 m. When the first signal is obtained, the coarse search starts.
- *Coarse search*. Approaching the area over the victim by following field flux lines that always pass through the transmitter. This stage finishes when the distance to the transceiver is approximately 4 m and the flux lines change direction rapidly because of their confluence.

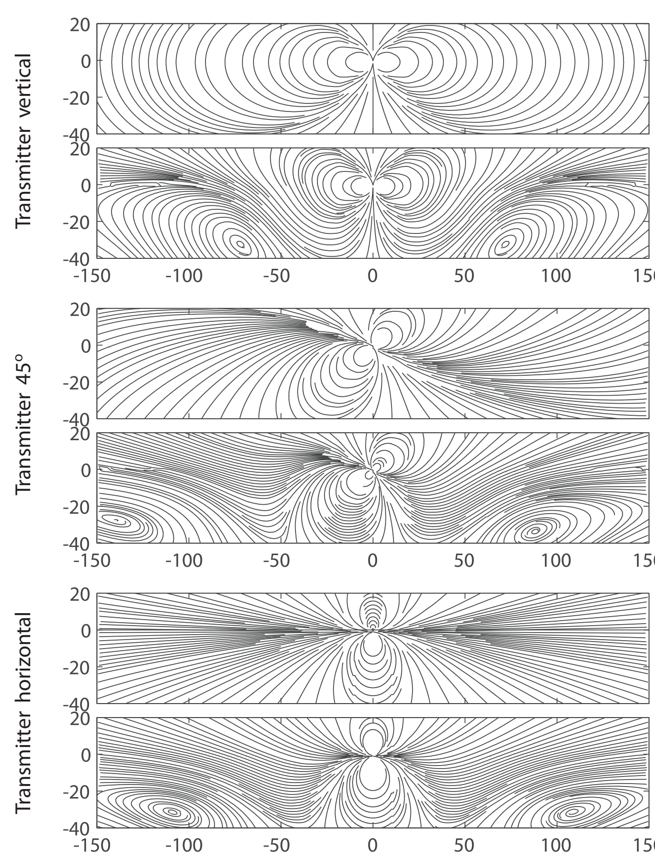


**Fig. 3.** Computed flux lines uniformly distributed at a vertical plane containing the dipole source buried at 1 m depth. The x-axis corresponds to the radial distance (in meters) to the source placed at 0. For any dipole orientation, the upper figure corresponds to the free-space and the down figure includes the soil effects.

- *Fine search*. Grid search slowly for the buried subject by searching the point of greatest signal strength within the approximated last 4 m. The transceiver must be held near the snow surface. A systematic approach can be the cross-like method; i.e., when the distance reading starts increasing (or the audible tone starts decreasing), the rescuer has to return to the point of least distance read (or maximum tone heard). Starting at this point, the rescuer has to take the perpendicular direction to get the lowest distance reading (or loudest sound turning down the volume to increase the searcher's sensitivity). The process has to be repeated until the distance reading is minimum (or maximum tone heard).

Some important aspects of the three search stages will be analyzed in the following sections. Firstly, the discussion will focus on the magnetic field pattern that can be distorted because of the snow and

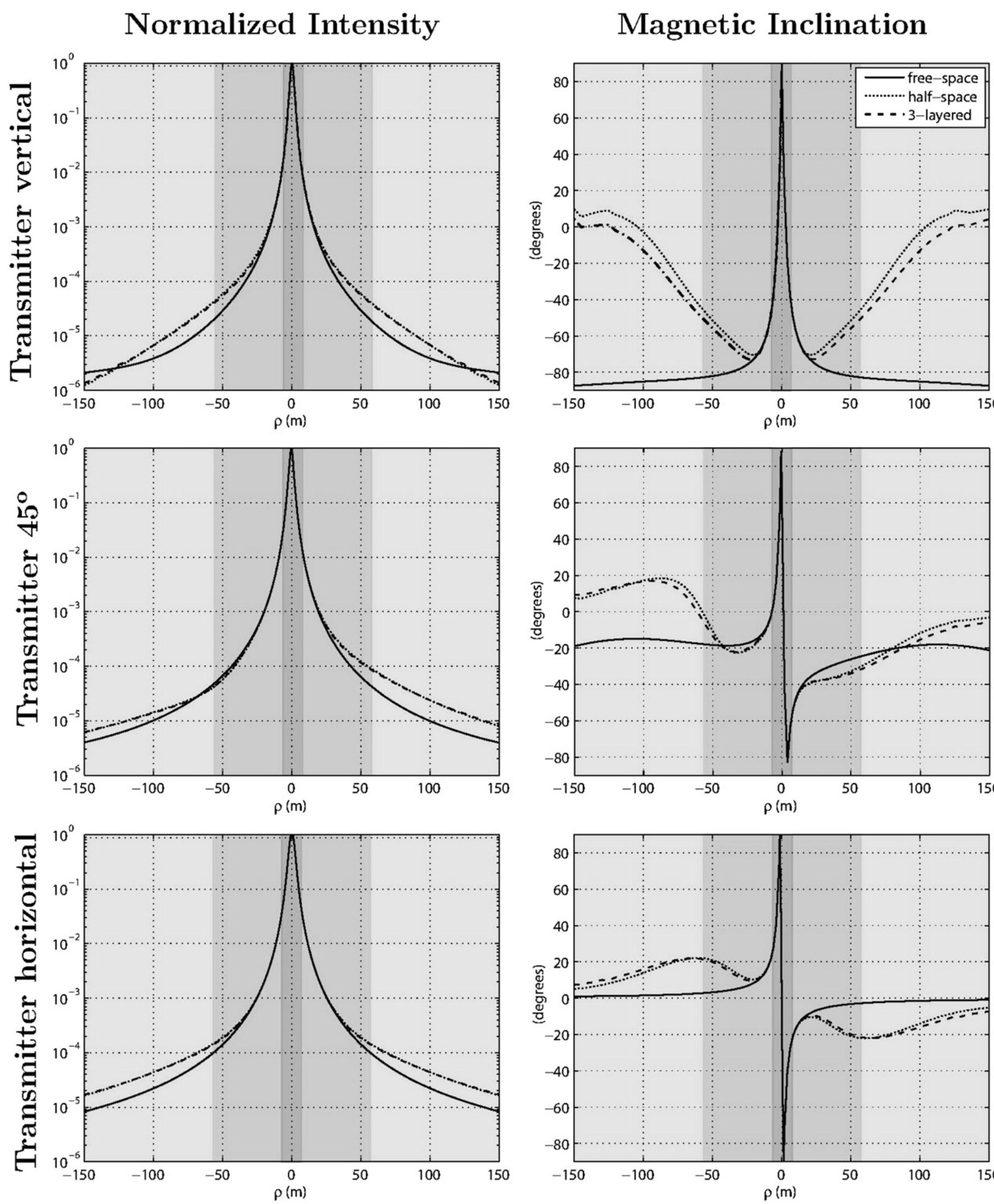


**Fig. 4.** Computed magnitude and inclination of the magnetic field along the *y*-axis to where the dipole source can be oriented at the signal/coarse search plane height. The range of each search stage is indicated: signal search (light gray), coarse search (medium gray) and fine search (dark gray).

soil media. Then, the maximum signal location with respect to the position over the buried subject will be analyzed.

## 3. Analysis of the magnetic field pattern

At the present time, all the searching strategies are based on the well-known near field magnetic field. Furthermore, the maximum field strength is assumed to be at the point on the surface closest to the buried subject.

This section analyzes the effects of the snow and soil media together with the field pattern for any source orientation. The problem was first considered by the authors in Ayuso et al. (2007).

### 3.1. Propagation models

Besides the simple approach of a magnetic dipole emitting in free-space, two refinement levels are considered:

- *Half-space*: with upper air and lower soil half-spaces.
- *Three-layered*: with upper air half-space, central finite depth snow layer and lower semi-infinite soil layer,

The soil and snow are modeled as linear, homogeneous, isotropic and horizontally stratified mediums.

See Fig. 2 for a general description of the problem and propagation models taken into account.

Regarding the model equations, the presence of a real boundary makes it necessary to explicitly consider the relative orientation of the emitting dipole. Thus, the source tilt is dealt with the addition of the fields generated by a vertical and a horizontal magnetic dipole of appropriate magnitude (Wait, 1982).

Since the pioneering work by Sommerfeld (1909, 1926), the electromagnetic fields from Hertzian dipoles in the presence of isotropic layered media have been calculated with analytical closed-form solutions by many researchers, in particular Prof. J.R. Wait (1961, 1969, 1972, 1982, 1996). Nevertheless, the formulations presented in the literature are disperse as the works have been focused on a particular dipole orientation, position and region of interest. Furthermore, because Sommerfeld integrals are involved, approximated formulae have been extensively derived due to the intricacy of evaluating their oscillating infinite nature. Therefore, the range of validity of the approximate solution has normally been limited to the near-region or the far-region. In this work, appropriate model equations valid for any distance range are derived and numerically validated. Appendix A includes the half-space formulation for the buried source and the observer placed in the air region. A comprehensive study can be found in Ayuso (2010).

### 3.2. Simulation parameters setup

The fields are expressed in terms of the complex permittivity $\varepsilon_c = \varepsilon_0 \cdot \varepsilon_r - j\sigma_{eq}/\omega$ of the medium. The real part, called the dielectric permittivity, is a measure of the polarizability of the dielectric molecules. The imaginary part accounts for the dielectric relaxation and electrical conductivity loss mechanisms. Then, $\sigma_{eq}$ is the equivalent conductivity and $\omega = 2\pi f$ is the angular frequency.

At the working frequencies of the avalanche transceivers, some representative electrical properties for common snow and soil media were established based on the literature and field measurements.

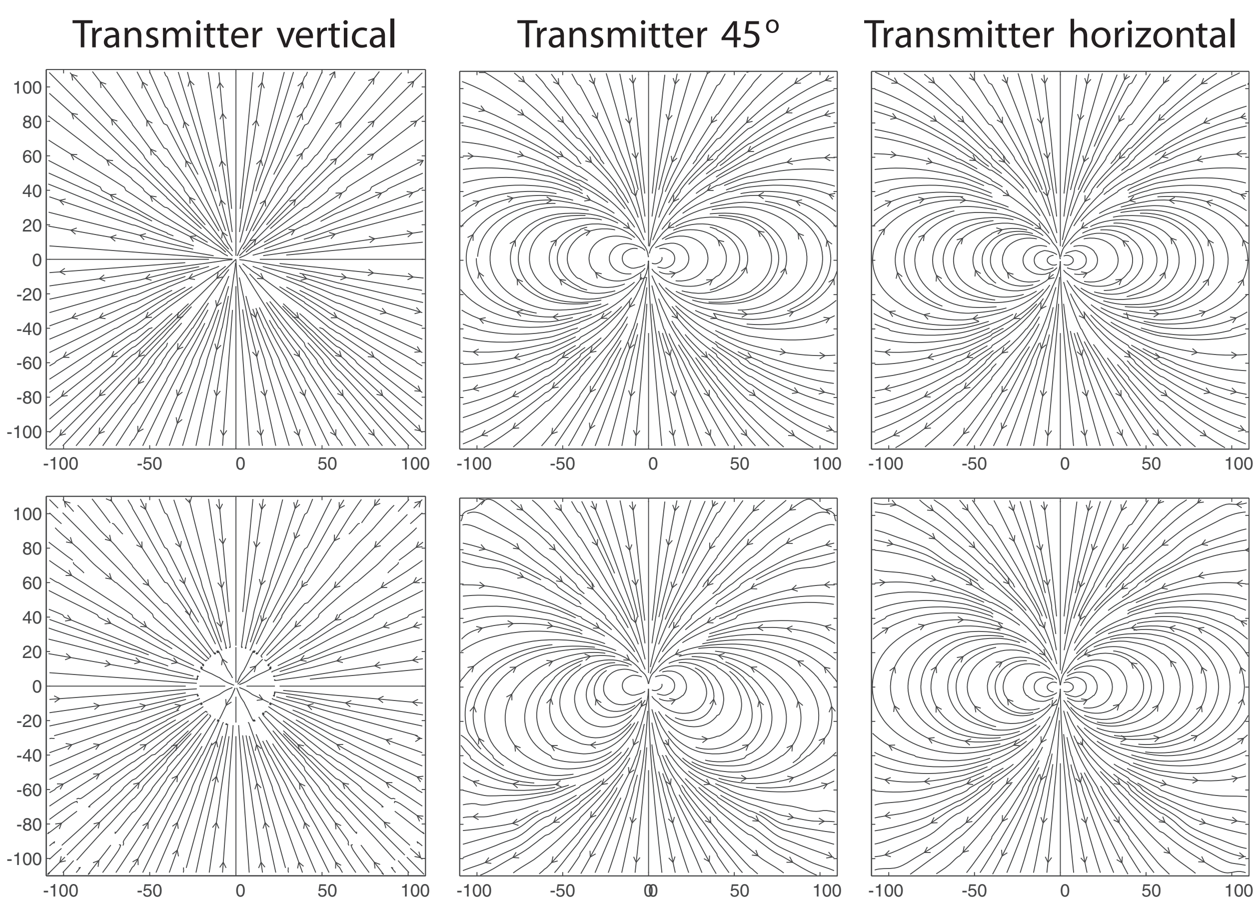


**Fig. 5.** Computed flux lines uniformly distributed at the signal/coarse search plane. Distances are in meters. For any dipole orientation, the upper figure corresponds to the free-space and the lower figure includes the soil effects.

The electrical conductivity of soil or rock is an extremely variable property that depends on the soil composition and water content. E.g. limestone or sandstone fall between 0.2 and 10 mS/m (Orellana, 1982). At 457 kHz, the equivalent conductivity is mainly due to the bulk conductivity. In contrast, the dielectric permittivity of soil depends only slightly on its chemical composition. The main contribution comes from the actual liquid water volume fraction present, with typical values close to 8 for the dielectric constant (relative dielectric permittivity) in a mildly wet soil (Keller, 1966).

Consequently, as the soil is assumed to be a moderately good conductor, the equivalent conductivity can be set to 1 mS/m and the relative permittivity to 8 according to the literature.

The snow mantle is an inhomogeneous mixture of ice, air and liquid water that behaves as a lossy dielectric (Colbeck, 1982). At the operation frequency of the avalanche transceivers, the effect of the detailed granular structure of the snow mantle on the electromagnetic field is negligible and it is possible to use homogeneous empirical mixing models for the estimation of the complex dielectric permittivity of the snow (e.g. Achammer and Denoth, 1994; Frolov and Macheret, 1999). Then, typical values of the relative dielectric permittivity span from 1.5 to 5, depending on the snowpack density and liquid water content. The equivalent conductivity due to the dielectric losses can be calculated following the guidelines of Herique and Kofman (1997). As a result, a value around 2 μS/m is obtained. The bulk electrical conductivity of snow was measured in the Pyrenees, Alps and Antarctica during a wide temporal distribution (Calvo et al., 2005). The resulting data showed that the DC bulk conductivity of the snow presented little variability around 1 μS/m.

Therefore, as high density mildly wet snow is considered, the equivalent conductivity is set to 3 μS/m (including both dielectric and conductivity losses). The relative permittivity is selected from typical values and set to 4.

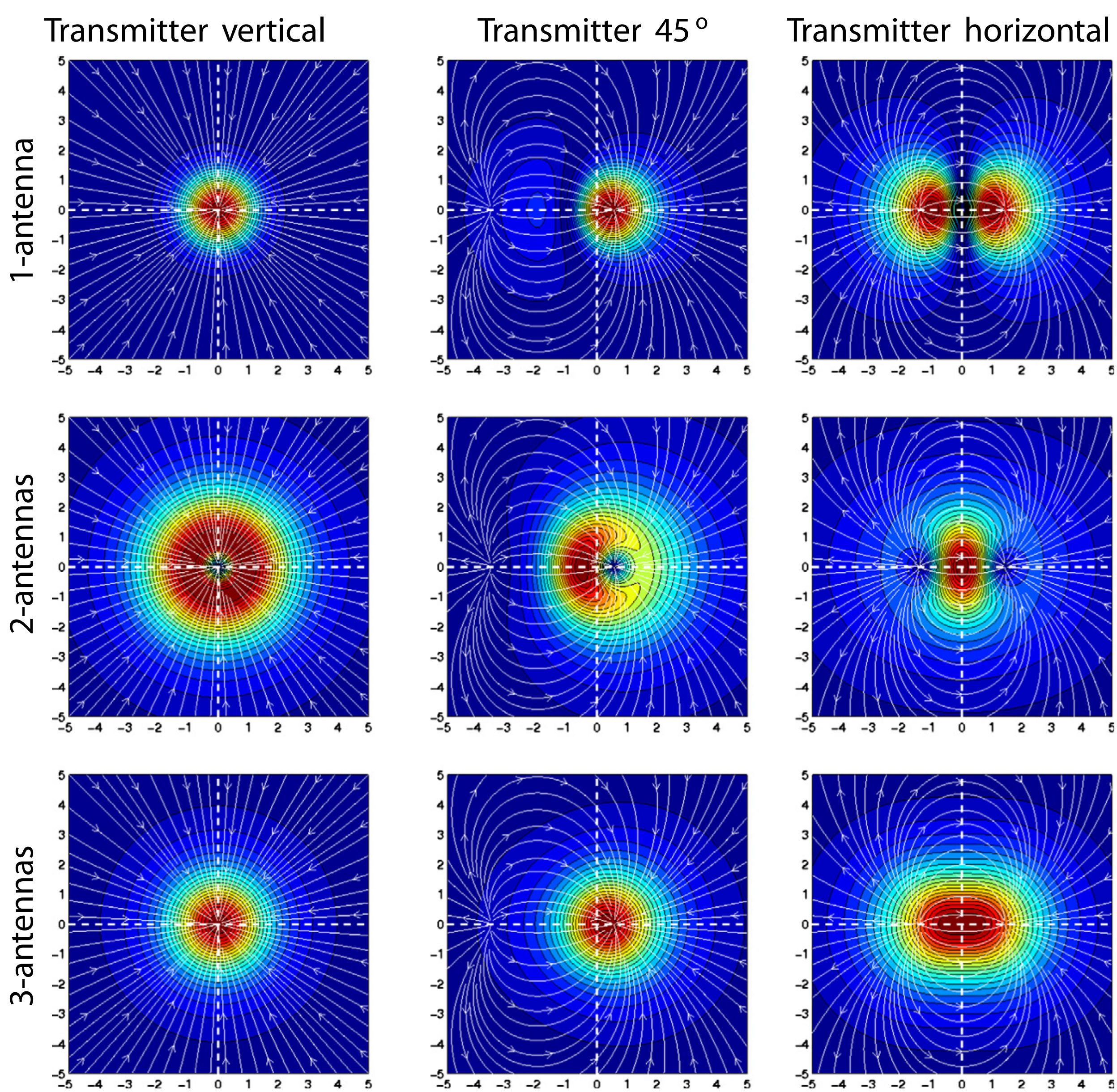


**Fig. 6.** Flow lines over the snow cover and intensity (lighter colors indicate higher signal intensity) of magnetic field sensed at the fine search plane by 1, 2 and 3-antennas transceivers for three inclinations of the emitting antenna: vertical, 45° and horizontal. The transmitting antenna is located in the center of each plot at a depth of 2m to highlight the effects.

The snowpack depth can vary from centimeters to tens of meters. In the simulations, the snow layer depth is set to 3 m in order to demonstrate its possible effects.

Finally, the transmitter is placed at a depth of 1 m, a mean value obtained from reported accidents (Falk et al., 1994).

Table 2 summarizes all the settings for the present simulations.

### 3.3. Magnetic field simulations

The analytical expressions have been numerically evaluated in the *MATLAB* environment with some additional work for stability and convergence related with the always difficult evaluation of the half-space and three-layered solutions as they involve Sommerfeld integrals (Siegel and King, 1970). The main difficulties are the truncation of the otherwise infinite integration variable and the oscillating nature of the integrand. These were resolved after a detailed study of the integrands.

This section will present the most relevant computed results for the models after studying three significant source orientations: vertical, horizontal and a tilt angle $\theta = 45°$.

Fig. 3 shows the computed field lines uniformly distributed at a vertical plane containing the dipole source. Therefore, according to the propagation models description (see Fig. 2), the x-axis corresponds to the radial distance to the source placed at 0. For any dipole orientation, the upper figure corresponds to the free-space model and the bottom figure takes into account the soil effects by means of the half-space model. The simulation results for the three-layered model have been omitted due to the negligible effects of the snow pack. As can be observed, there are important differences between the physics of the free-space problem and the half-space problem. They arise because of secondary magnetic field due to eddy currents, i.e. the electric currents induced by the oscillating magnetic field in the conducting earth, and the effect of the air–earth interface.

In free-space, magnetic field falls within the near field region. As a result, radiation can be ignored. In the half-space model, part of the field is in the free-space and part in a lossy medium. In the latter, radiation starts to be evident because the secondary magnetic field begins to be noticeable. The near field limit is reduced because the medium can be considered a good conductor for the simulation parameters set-up. Therefore, the near field limit is given by the skin depth of the medium, i.e. 23.5 m. Notice that the conductivity of the soil directly determines where the near/far field region is placed. Consequently, this limit will be increased or reduced according to the equivalent conductivity of the soil affected by the melting of the snow pack.

Fields in the air are due to the fields transmitted from the buried dipole through the air–soil interface. As the tangential component of the field has to be continuous, fields in the air region can deviate from those of the free-space model predictions to a greater or lesser extent depending on the source inclination. This will be further analyzed in the following.

To sum up, while the fine search takes place close to the transmitter and thus, inside the near field range, this is not the case for the signal and coarse searches. These stages are carried out farther from the source, at distance ranges where strong deviations from the near field case are expected due to the ground conductivity.

Fig. 4 shows the computed magnetic field intensity normalized to maximum value and the inclination of the field for any source orientation. On the one hand, the analysis of the simulation results reveals that adding the snow layer does not introduce significant differences to the half-space model under the avalanche rescue conditions. On the other hand, there are marked differences between the free-space and half-space models, mainly in the inclination of the field, in the signal and coarse search areas. Notice how in the case of the vertical transmission, the field is no longer vertical but tend to lay along the air–soil interface. Therefore, search strategies based on field measurements in these regions must be interpreted according to the half-space propagation model in order to avoid erroneous inferences.

In the end, Fig. 5 shows the aforementioned field lines that are usually followed in order to approach the victim. For clarity, the magnitude of the field is not depicted by the density of field lines. As can be seen, the axial symmetry of the flux lines for the vertical orientation is invariant with the propagation model although the direction is reversed at approximately 20 m from the position over the source due to the transition from the near region to the far region (see Fig. 3 to observe the field lines along the *x*-axis at the search plane height). As a result, the horizontal component of the field can be missed during the coarse search due to its zero-cross. Finally, notice that the path formed by the flux lines leads directly to the source. The 45° inclination case shows noticeable differences between the models but without effects on the search. In addition, there are imperceptible differences between the 45° and the horizontal inclinations for the free-space model. This is due to the horizontal component of the field for the vertical transmitter is much lower than the horizontal component of the field for the horizontal transmitter and the uniform representation of the field. Lastly, the horizontal case presents no change in the distribution of the flux lines with the propagation model.

Finally, notice that this plot does not give enough resolution in the region concerning the fine search. See Fig. 6 for a detailed plot of the field lines distribution and the field strength in the vicinity of the buried emitter. As can be seen, the points where the directions converge can be roughly apart the burial location. In addition, in case of a non-vertical transmitter, they do not converge at a single point. However, this can be disregarded as the field strength is also used for locating the buried source. The location accuracy will be analyzed in the following section.

## 4. Analysis of location accuracy

The search by avalanche transceivers depends on the magnetic field generated by the emitting device, how the magnetic field propagates and how it is perceived by the receiving device. Considering only the final stages of the search (the final part of the coarse search and the fine search), it can be assumed that the magnetic field is not distorted by the medium (see Section 3) and is correctly described by the vacuum equations. Then, the magnetic field perceived is affected by the number of orthogonal antennas placed in the receiver. Therefore, the following analysis of the location accuracy is accomplished from the perspective of the number of receiving antennas taking into account that location takes place within the third antenna range.

Nowadays, the coarse search is performed following the flux lines over the snow surface. For one antenna unit, the device is horizontally

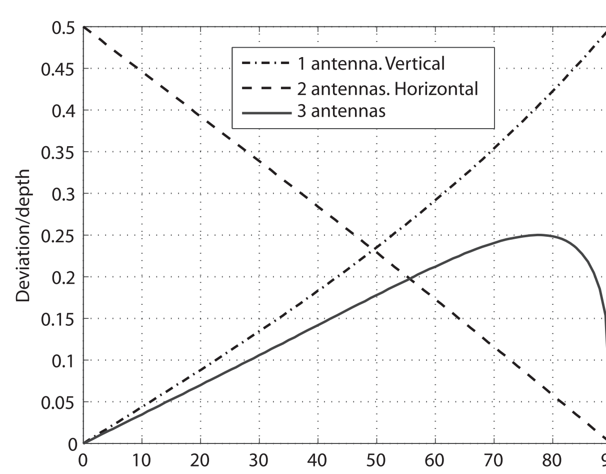


**Fig. 7.** Location error depending on the burial depth and the transmitter inclination from vertical.

placed and rotated looking for the maximum signal which coincides with the direction of the flux lines. For the rest of the transceivers, the direction of the flux lines is displayed as directional arrow. In this way, the rescuer reaches the vicinity of the buried subject and then the fine search starts. The fine search is performed finding a maximum of the signal or a minimum of the distance to the transmitter (see Section 2). The one-antenna transceiver has to be brought upright. Otherwise, depending on the direction of the approach, the location of the maximum is different, making the search unfruitful. Two and three-antennas units are carried horizontally during all the stages of the search. Furthermore, be aware that even despite the transceiver is properly carried, one and two-antenna transceivers can detect multiple maximum signal in deep burials. This is illustrated in the following.

Fig. 6 shows a simulation of the flow lines and the magnetic field strength as perceived for each type of avalanche transceiver. Now the source depth has been increased to 2 m to enhance the visualization of the effects of the source inclination. Observe how the maximum strength of the magnetic field is not always situated over the source, and that it may cover a wide area. Consequently, a precise location of the maximum does not always represent an accurate victim location. In addition, there could be more than one maximum. See for example the computations for the transmitter tilted at 45° and the 2-antenna receiver where there are two zones of maximum signal. Fortunately, this problem can be overcome by using receivers with three mutually orthogonal antennas.

Finally, the exact position (*MaxPos*) of the maximum of the normalized magnetic field (*NormH*) in relation to the burial depth (*depth*) was computed for every source inclination (*inclination*) for one, two and three-antenna receivers following the algorithm:

**for** inclination 0 to 90° **do**
  $H_x, H_y, H_z \leftarrow \mathrm{H}(\text{inclination, depth})$
  $H_{1\text{ - antenna}} \leftarrow |H_z|$
  $H_{2\text{-antennas}} \leftarrow \sqrt{H_x^2 + H_y^2}$
  $H_{3\text{-antennas}} \leftarrow \sqrt{H_x^2 + H_y^2 + H_z^2}$
  **for** n = 1 to 3 **do**
    $NormH_{\text{n - antenna(s)}} \leftarrow H_{\text{n - antenna(s)}} / max(H_{\text{n - antenna(s)}})$
    $MaxPos_{\text{n - antenna(s)}} \leftarrow \mathrm{find}(NormH_{\text{n - antenna(s)}} \geq 1 - \mathrm{eps})$
  **end for**
**end for**
plot(inclination, $MaxPos_{\text{n - antenna(s)}}$ / depth)

where the function *H* computes the Cartesian components of the magnetic field, the function max returns the largest value of the argument, the function *find* returns the position of the values that guaranteed the condition passed in the argument and *eps* is the floating point relative accuracy of the machine.

As a result, the displacement with respect to the location over the transmitter depends on the source tilt and the type of receiver. Fig. 7 shows the simulation results. As can be seen, for three-antenna transceivers, the location error is limited to 25% of the burial depth whereas for one or two-antenna transceivers, the error can be increased to 50% of the burial depth. Then, a victim buried at 2 m could be located 1 m away if one or two-antenna transceivers are used whereas this error would be reduced to 0.5 m for three-antenna units. Furthermore, a vertical transmission is the best case for one and three-antenna receivers as the location error is minimum. Nevertheless, this is the worst case for two-antenna receivers. However, one and three-antenna transceivers are the most commonly used devices, the former because of their lower price and the latter because they avoid the problem of having more than one maximum signal for a third antenna range of at least 5 m (Schreilechner et al., 2010) and they incorporate the latest technological advances for assisting the search.

To sum up, the present study reveals that there is an error associated with the method of searching for the maximum signal that depends on the source tilt and burial depth for any type of transceiver. The three-antenna transceivers are the most accurate with location errors below 25% of the burial depth. Finally, vertical transmission is the best case for locating an avalanche victim as the location error is minimum for the most popular transceivers.

## 5. Field experiments

In the previous sections, the search by avalanche transceivers has been theoretically analyzed. However, there are factors that are difficult to take into account from a theoretical point of view. These factors are related with the rescuer–device relationship and depend on how the information is shown, the rescuer experience and so on. The influence of these kinds of factors was estimated by a set of field experiments conducted in the Formigal ski resort (Pyrenees, Huesca, Spain).

### 5.1. Experiment one

The first experiment, carried out in January 2010, was designed with the following objectives:

1. To establish the best way to keep the transceiver during the signal search.
2. To measure the actual error in the victim location during the fine search.

**Fig. 8.** Experiment one. Rescuers completing the fine search and differential GPS geo-referencing works of the marked location.

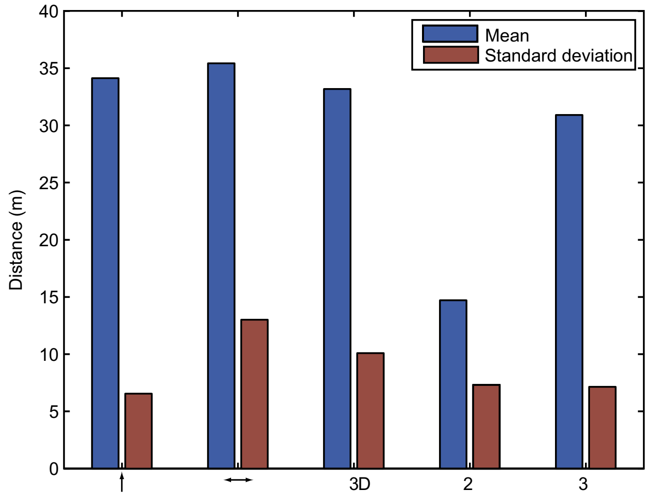


**Fig. 9.** Experiment one. Distance of the first signal from the transmitter: ↑. Vertical one-antenna device; ↔. Horizontal scanning one-antenna device; 3D. 3D movements one-antenna device; 2. two-antenna device and 3. three-antenna device.

The working group consisted of 25 people including specialists in avalanche rescue from the Mountain Service of the Guardia Civil, the Mountain and Special Operations School of the Spanish Army and the Formigal ski resort patrol. For this experiment a hillside area was selected. The transmitters were arranged in horizontal, vertical and 45° orientations at the bottom of a trench of 2.30 m depth. Fig. 8 shows the transmitter site and the personnel involved in the field works. A total of 23 avalanche transceivers of different brands and models were used as receivers: 9 one-antenna, 4 two-antenna and 10 three-antenna. A differential GPS with a base station placed in the ski resort allowed sub centimeter precision to geo-reference the relevant locations of the test.

For the first objective, in the case of one-antenna avalanche transceivers, three different strategies were tested: keeping the device vertical (↑), horizontal scanning (↔) and movement along the three spatial directions (3D). In case of digital transceivers of two and three-antennas, the devices were kept horizontal because this is the current orientation in the coarse search. The distance from the transmitter to the point with the first usable signal (the beginning of the next search phase) was measured for all the avalanche transceivers, for the three transmitter positions and for three directions of approach (in the same direction, at 45° and perpendicular to the transmitter antenna axis).

Fig. 9 presents the statistics of this signal search experiment. The horizontal scanning (↔) presents the best mean average performance for one-antenna devices. The results are improved if the particular case of the vertical transmitter is omitted as the magnetic field is mainly vertically oriented. Therefore, horizontal scanning performs like the other strategies in the quite representative field tests of the experiment. As it represents the simplest transition between the signal and coarse

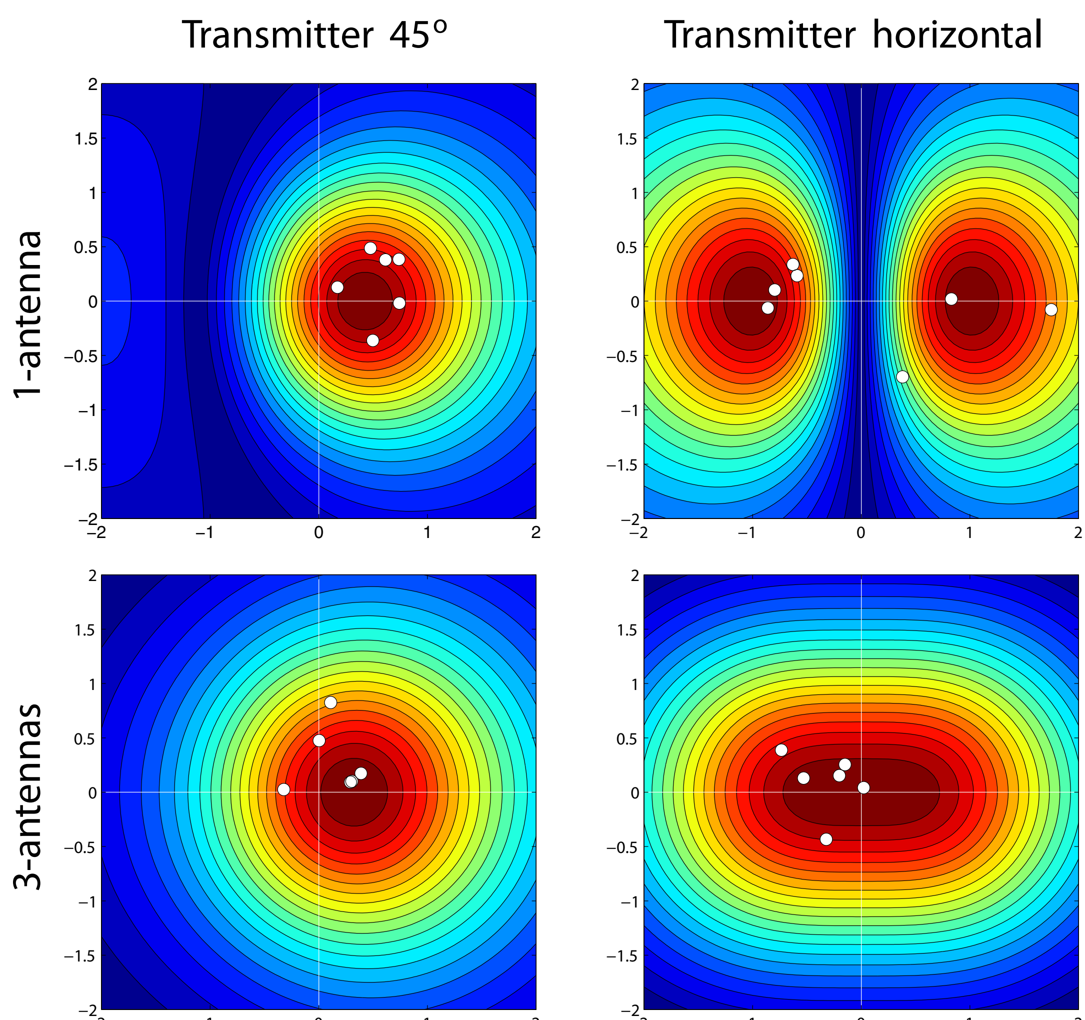


**Fig. 10.** Experiment one. Black dots represent the final positions over the buried subject located by professional rescuers (distances are in meters). The transmitter is located in the center of the figure. Computed magnetic field intensity as sensed by one and three-antenna receivers (lighter colors indicate higher signal intensity) at the fine search plane.

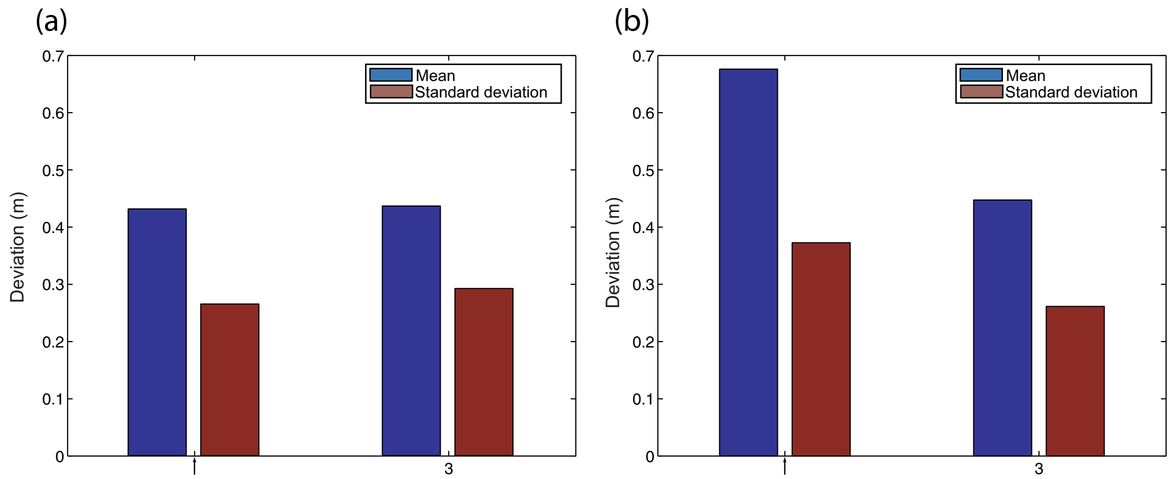


**Fig. 11.** Experiment one. subfig:MaxError Error in the location of the maximum signal, and subfig:VictimError Error in the location of the victim.

search phase, we recommend horizontal scanning for one-antenna transceivers during the signal search.

The three-antenna transceivers (3) behave similarly to those of one-antenna, although slightly worse. This is because they need a better signal for the digital processing and calculation of the direction and distance (in this case the transition between the two phases is decided by the device). It is worth noting that the two-antenna devices used in the experiment showed unexpected much worse results than the others. The consequent analysis of the two-antenna transceivers showed evident functioning problems in half of the used units (2/4). Therefore, the conclusions of the following experiment are only valid for one and three-antenna transceivers.

For the second goal, the position of the maximum signal has to be determined. The coarse and fine search was performed from different approach directions. The experiment was repeated for the transmitter in vertical, horizontal and 45° oriented positions for one and three-antenna receivers. It was observed that the peaks detected by one-antenna transceivers in the upright position and the three-antenna transceivers are close to the theoretical maximum location. Fig. 10 shows graphically some results of the experiment.

To conclude, Fig. 11 shows the errors with respect to the maximum location and the position over the victim for one-antenna and three-antenna devices. The results showed the same mean performance in locating the signal maximum (see Fig. 11a). This outcome shows that three-antenna devices that incorporate technological advances based on digital technology that are supposed to facilitate their use by rescuers, does not mean that the absolute accuracy has also been improved. This is further analyzed in the second experiment described below. Finally, Fig. 11b shows the errors with respect to the victim position. As expected, three-antenna devices have minor errors, the maximum signal being closer to the buried subject.

### *5.2. Experiment two*

A second experiment, carried out in March 2010, was designed with different objectives. Here, we focus on the location error by one and three-antenna receivers using the cross-like method.

The experiment involved four dummies used as buried subjects, see Fig. 12. The dummies were buried at an average depth of 1.50 m (maximum depth of snow pack that day), in four different orientations, i.e. vertical, horizontal, 45° and 63°. Remotely activated transmitters were used to avoid signal interferences. Up to 15 complete blind searches were performed with one and three-antenna transceivers.

During the field work, the position of the maximum established in the search was measured. Then, the error in the location, being the distance to the location over the buried subject, was calculated. As a result, on the one hand the one-antenna transceivers presented a mean error of 0.38 m (standard deviation 0.25 m). On the other hand, the three-antenna transceivers presented a surprising mean error of 0.74 m (standard deviation 0.21 m), greater than the error of the one-antenna transceivers. This discrepancy with what was initially expected prompted a subsequent study.

The hypothesis for explaining this result was related with the precision in the representation of the distance. All the transceivers used in the experiment represented the distance with a resolution of 0.10 m. Thus, the maximum signal (minimum distance) is perceived as circular or ovoid shapes with a non negligible area. To confirm this hypothesis, a simulation of the calculus and representation of the distance for the experiment was performed. Fig. 13 shows the simulation results. As can be seen, the final points of the search are placed at the boundary of the formed area.

Therefore, the conclusion is that the cross search technique is not the best suited when signal maxima are perceived not as points but as surfaces with a non negligible area. The following section presents a validated technique that finds the center of the formed figure and, consequently, can significantly reduce the location error.

## 6. Improving the search

### *6.1. The perpendicular bisector method*

Taking into account that three-antenna avalanche transceivers can determine a minimum distance flat region of considerable dimensions for burial depths greater than 1.5 m, the fine search strategy should be adapted to this situation. Thus, a new search strategy directed not to find a minimum distance (maximum signal), but the center of one flat geometrical figure (see Section 5.2) is proposed and subsequently evaluated. Fig. 14 shows the proposed strategy, called the perpendicular bisector method for a burial depth of 1.5 m and a distance resolution of 0.1 m. The idea is to finalize the cross-based search finding the center of the minimum distance figure. Firstly, a segment with the shortest distance is located (segment 1). The segment limits (black dots) coincide with the border of the figure of minimum distance. Then, a perpendicular line is drawn through the midpoint of the segment. With this new line, the process is repeated (segment 2). The center of the third segment (second bisector) is an estimation of the geometrical center of the minimum distance figure (white dot).

This method was evaluated in a new definite experiment conducted in April 2010. The experiment consisted of multiple fine searches with three-antenna receivers. The transmitter was located at different inclinations up to an extreme depth of 3 m. As a result, the average location error, from the position marked as the maximum signal or the minimum distance to the victim, was 0.32 m. Notice that in experiment two, the location error was 0.74 m for an average burial depth of 1.50 m using the cross search method. Moreover, if we omit from both experiments the particular case of the horizontal transmitter, the results are even better. The location error is reduced to 0.13 m for the new technique in comparison to 0.51 m for the classical cross search. However, the implementation of the proposed method turned out to be more complicated than the conventional grid search. Therefore, training is mandatory for a real benefit of the proposed technique.

To conclude, a method of determining the center of a circular, elliptical or ovoid figure that represents the minimum distance to the victim or maximum signal has been presented. It has been experimentally demonstrated that the perpendicular bisector method notably improves the classical cross search technique accuracy.

### 6.2. Vertical transmission

As a result of the analysis of the magnetic field pattern and the location accuracy (see Sections 3 and 4, respectively), we are considering the special case of forcing vertical transmission to improve the search by avalanche transceivers. This forced vertical emission mode will maintain the compatibility with existing receivers and complies with the standard. In the following, its effects on every stage of the search are discussed.

During the signal search, the maximum realistic range determines the search strip width recommended by manufacturers. Thus, range reduction will affect the time spent on signal search. Presently, only the horizontal component of the field is sensed. Despite three-antenna transceivers have an antenna oriented in the $z$-axis, this only works on the fine search phase close to the transmitter because of its limited sensitivity. We have computed the maximum achievable range when the transmitter is vertical and horizontal for the free-space and half-space propagation models taking into account the simulation parameters of Section 3.2. As a result, Fig. 15 represents the area delimited by the calculated signal sensitivity of 20 nA/m for existing transceivers that only sense the horizontal field and future transceivers that would be able to sense the full field components. These results are comparable with recent experimental range measurements (Hellberg et al., 2014).

As can be seen, maximum range reduction for the vertical transmission is about 53% for the free-space and 42% for the half-space propagation model. If the $z$ component of the field is also sensed, range reduction is decreased to the 27% and 20% respectively. In conclusion, range can be significantly reduced for the vertical transmitter when only the horizontal components of the field are sensed. Notice that absolute ranges are higher for the half-space propagation model, closer to the real scenario.

Nevertheless, nowadays, the recommended search strip width based on field tests is much lower than the value derived from the maximum range. As range reduction due to the transmitter–receiver relative orientation and propagation effects should be considered. Then, a search strip width of 20 m must be used to avoid missing any victim in the signal search. Consequently, such a search strip width is adequate in case of a vertical transmission. However, the signal search time could be increased due to the lower range.

Concerning the coarse search, this could be more affected due to the vertical transmission field pattern. When field lines are close to vertical, direction indication finds problems due to the little projection onto the $x$ and $y$ antenna axis. As a result, the range the signal may be effectively traced towards the transmitter can be significantly decreased. However, in practice, the field is tilted due to the effects of the soil and also when the search takes place at different elevations in a sloping surface. Anyway, due to the axial symmetry of the field pattern, an approach method rather than following the field lines but based on the geometry of the field could be used to overcome the problems due to the small horizontal field component. Since the middle of the last century a buried vertical oscillating magnetic dipole has been used to establish the surface point in its axis (radiolocation). Proposed methods have reported an accuracy of 3% of the burial depth (see Ayuso et al., 2010). Thus, the well-known geometry of the magnetic field for the vertical transmitter could be used to define a specific coarse search method to be used in the forced vertical emission case.

Finally, the fine search specially improves using the proposed vertical transmission. This is the most time consuming, complex and stressing task. According to Matzner (2008), the transceiver should indicate the true position of the transmitter as accurately as possible, regardless of the orientation of the transmitter's antenna. We have demonstrated

**Fig. 12.** Experiment two. Recovered dummy with remotely activated avalanche transceiver transmitter.

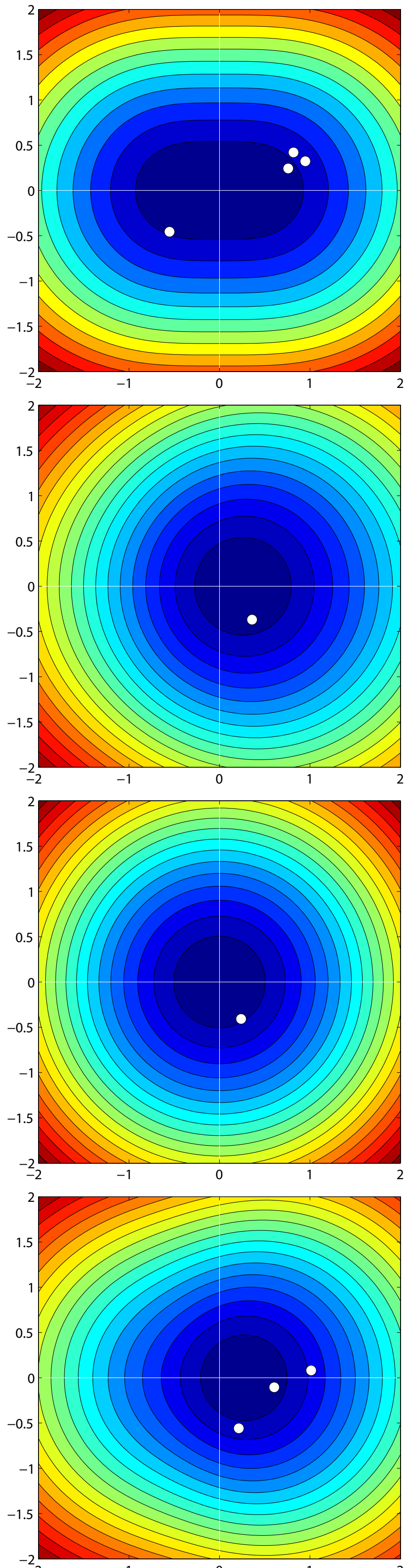


that the location error due to the displacement of the position of the maximum signal over the victim is minimal when the transmission is accomplished close to the vertical inclination. Besides, a very localized maximum is obtained and the reduction in the degree of localizability due to the burial depth is thus minimized.

Unfortunately, the development of the proposed method is a technological and industrial challenge. Contemporary devices need to be redesigned to overcome an existing limitation, i.e., the short *z*-antenna length due to the dimensional restrictions of the housing. This means that in order to satisfy the standard, a very high current would be needed giving rise to a prohibitive power consumption. Therefore, only a breakthrough into the present avalanche transceiver design that allows an enlarged *z*-antenna could overcome this serious problem.

In addition, forced vertical transmission requires additional circuitry that will imply an increase of manufacturing costs.

## 7. Conclusions

Avalanche transceiver search is based on the near field magnetic field pattern. The influence of the snow and soil media has been studied with the half-space and three-layered propagation models. This paper presents the computation results for realistic parameters setup. To sum up, the air–soil interface has noticeable effects in the regions concerning the signal and coarse search while the near field limit perfectly describes the avalanche transceiver field pattern during the fine search.

The location of the victim is usually determined from the maximum signal sensed. If only the maximum signal displacement from the position over the victim is considered, the location error depends on the source inclination and depth and the number of antennas of the receiver. Computations show that receivers with three antennas when all of them are working are the most accurate, give an error below 25% of the burial depth. For one and two-antenna receivers the error can reach up to 50% of the burial depth.

The search by avalanche transceivers has been also analyzed by comprehensive field experiments. As a result, the useful range of one and three-antenna transceivers was found to be very similar. Besides, the strategy of horizontal scanning showed slightly better useful range than the other search strategies for one-antenna transceivers and this also facilitated the transition from the signal to the coarse search phase. As theoretically predicted, the lowest location error corresponded to three-antenna receivers. Moreover, they presented similar maximum signal location errors as one-antenna receivers. The consequent study showed that this is due to the distance resolution. As the maximum is perceived as a plane figure, the cross-like method can perform inefficiently in case of deep burials because the maximum location is placed at the boundary of the figure.

Consequently, a new final search strategy, called the perpendicular bisector method has been proposed and put into practice experimentally. This locates the center of the formed figure. As a result, the location accuracy can be significantly improved. Training on the new technique would be required in order to take advantage of this extra accuracy without the need for additional search time.

Furthermore, based on the analysis of the magnetic field pattern and location accuracy, forced vertical transmission of the avalanche transceiver has been proposed as an additional improvement. As it is well-known, the range in vertical emission mode is significantly reduced in comparison with the horizontal transmission. However, the main problem can arise during the coarse search because of the very limited horizontal field. But this can be overcome as the field pattern is well-known by means of a different search technique using the forced geometry.

**Fig. 13.** Experiment two. White dots represent the final positions over the buried subject located by professional rescuers using three-antenna transceivers (distances are in meters). The transmitter is located in the center of the figure. From top to bottom: transmitter horizontal, 45°, vertical and 63°. Computed distance to the transmitter as is calculated and displayed (lighter colors indicate greater distances) at the fine search plane.

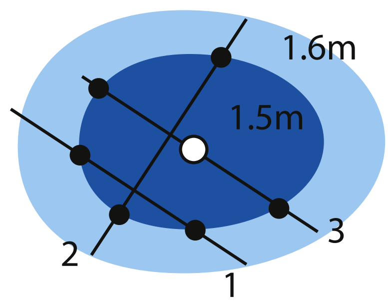


**Fig. 14.** Scheme of the perpendicular bisector method. Three segments (limits marked by black dots) can determine the center of the figure of minimum distance (marked by a white dot).

Finally, the fine search phase would be specially improved as the location error is minimized using currently available search strategies and transceivers. Unfortunately, the implementation of the forced vertical emission operation mode is a technologically and industrially challenging task. Therefore, a breakthrough into current designs with the participation of avalanche transceiver manufactures is imperative.

To conclude, the present theoretical and experimental works have involved the real operation of avalanche transceivers. A deeper knowledge of the core of the search has thus been achieved. The new proposals presented in this paper aim to improve the search process and then lead to an increase in the chances of survival after an avalanche.

**Acknowledgment**

The authors would like to thank to the reviewers for their valuable comments that have contributed to improve the quality of the paper. In addition, the authors would like to specially thank to Mr. Felix Meier for his thorough comments highlighting the vertical transmission technological and industrial problems. We would like to thank the Aramon Group and the Formigal ski resort for the use of their facilities and the inestimable support of the staff for conducting the experiments.

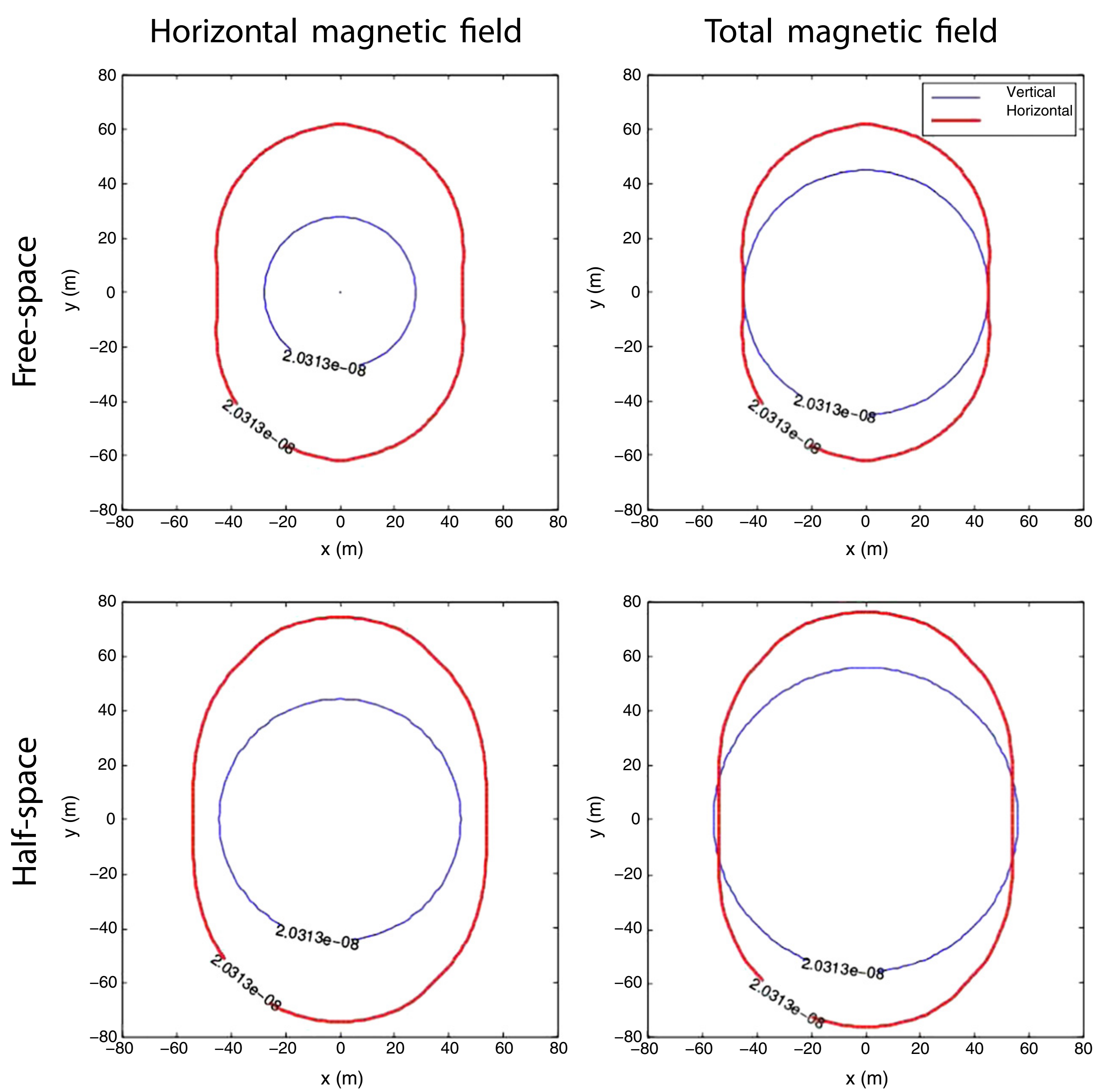


**Fig. 15.** Range computations for an estimated sensitivity of 20 nA/m for a vertical and a horizontal transmitter.

In addition, our thanks go to the members of the Escuela Militar de Montaña y Operaciones Especiales (EMMOE) of the Spanish Army, Servicio de Montaña de la Guardia Civil of the Dirección General de la Guardia Civil, the University of Zaragoza and Peña Guara Mounatin club for their help with the field tests and Rafael Larma for his inestimable topographical work. This research was partially supported by the Aragón Government (Aragón, Spain) under Project "Grupo DGA T04-FSE".

## Appendix A. Half-space formulation

In Fig. 2, a general description of the problem in spherical coordinates is illustrated. In free-space, the electrical properties of the medium are $\varepsilon = \varepsilon_0 \simeq 8.854 \times 10^{-12}$ F/m and $\mu = \mu_0 = 4\pi \times 10^{-7}$ H/m. The air occupies the region $z \geq 0$ where $\sigma = 0$ S/m. The interface at $z = 0$ is the upper edge of a homogeneous ground of conductivity $\sigma_1$ and relative dielectric constant $\varepsilon_{r1}$. Free-space permeability is assumed everywhere, $\mu_0$. The magnetic dipole is situated on the $z$-axis at a depth $z_e$ and the magnetic fields are calculated at any point in the air region.

The solutions for the vertical source when the dipole is oriented in the $z$-direction are derived in cylindrical coordinates $(\rho, \phi, z)$, with base vectors $(\hat{\rho}, \hat{\phi}, \hat{\mathbf{z}})$, due to the symmetry of the problem. The horizontal source is oriented in the $y$-direction and the Cartesian coordinate system $(x, y, z)$ with base vectors $(\hat{\mathbf{x}}, \hat{\mathbf{y}}, \hat{\mathbf{z}})$ is used. The solutions of an arbitrary inclined transmitter with respect to the $z$-direction can be calculated from the decomposition of the dipole into the equivalent sum of a horizontal and a vertical dipole in the Cartesian coordinate system.

In addition, the well-known geometric relations between coordinates and unit vectors allow the coordinate system of the solutions to be changed.

Then, for the vertical dipole source the fields are determined by,

$$H_\rho = \frac{M}{4\pi z_e^3}\int_0^\infty \lambda' z_e u_0 A e^{-u_0 z} J_1\left(\frac{\lambda'}{z_e}\rho\right) d\lambda' \tag{A.1}$$

$$H_\phi = 0 \tag{A.2}$$

$$H_z = \frac{M}{4\pi z_e^3}\int_0^\infty \lambda'^2 A e^{-u_0 z} J_0\left(\frac{\lambda'}{z_e}\rho\right) d\lambda' \tag{A.3}$$

where $z_e$ is the burial depth of the source. The variable of integration is defined as $\lambda' = \lambda \cdot z_e$ for numerical work and the transmission is accounted for

$$A = \frac{2u_1}{u_1 + u_0}\frac{\lambda'}{z_e}\frac{1}{u_1}e^{-u_1 z_e} \tag{A.4}$$

where $u_n = \sqrt{\lambda'^2/z_e^2 - k_n^2}$ for any media given the wave number, $k_n$. In vacuum, $k_0 = \omega\sqrt{\mu_0\varepsilon_0}$. For the soil, $k_1 = \omega\sqrt{\mu_0\varepsilon_{c_1}}$. where $\varepsilon_{c_1} = \varepsilon_0\varepsilon_{r_1} - j\sigma_{eq_1}/\omega$ is the complex permittivity of the medium.

For the horizontal source, the fields are expressed by,

$$H_x = \frac{M}{4\pi z_e^3}\int_0^\infty (-A + u_0 R) e^{-u_0 z}\frac{\lambda' z_e x y}{\rho^2}\left(\frac{\lambda'}{z_e}J_0\left(\frac{\lambda'}{z_e}\rho\right) - \frac{2}{\rho}J_1\left(\frac{\lambda'}{z_e}\rho\right)\right) d\lambda' \tag{A.5}$$

$$\begin{aligned} H_y = & \frac{IdA}{4\pi z_e^3}\int_0^\infty (h^2 k_0^2 A e^{-u_0 z} J_0\left(\frac{\lambda'}{z_e}\rho\right) + \\ & +(-A + u_0 R) e^{-u_0 z}\left(\frac{\lambda'^2 y^2}{\rho^2}J_0\left(\frac{\lambda'}{z_e}\rho\right) + \lambda' z_e\left(\frac{1}{\rho} - \frac{2y^2}{\rho^3}\right)J_1\left(\frac{\lambda'}{z_e}\rho\right)\right)\Bigg) d\lambda' \end{aligned} \tag{A.6}$$

$$H_z = \frac{M}{4\pi z_e^3}\int_0^\infty \left(u_0 A - \frac{\lambda'^2}{z_e^2}R\right) e^{-u_0 z}\frac{\lambda' z_e y}{\rho}J_1\left(\frac{\lambda'}{z_e}\rho\right) d\lambda' \tag{A.7}$$

where

$$A = \frac{2k_0^2 u_1}{k_0^2 u_1 + k_1^2 u_0}\frac{k_1^2}{k_0^2}\frac{\lambda'}{z_e}\frac{1}{u_1}e^{-u_1 z_e} \tag{A.8}$$

$$R = \frac{2u_1}{u_1 + u_0}\frac{k_1^2 - k_0^2}{k_0^2 u_1 + k_1^2 u_0}\frac{\lambda'}{z_e}\frac{1}{u_1}e^{-u_1 z_e}. \tag{A.9}$$

## References


Achammer, T., Denoth, A., 1994. Snow dielectric properties: from DC to microwave X-band. Ann. Glaciol. 19, 92–962.

Ayuso, N., 2010. Modeling and Applications of Through-the-Earth Magnetic Field Propagation. (Ph.D. thesis). University of Zaragoza.

Ayuso, N., Cuchí, J.A., Lera, F., Villarroel, J.L., 2007. Avalanche beacon magnetic field calculations for rescue techniques improvement. International Geoscience and Remote Sensing Symposium. Barcelona, Spain, July 23–27, pp. 722–725.

Ayuso, N., Cuchí, J.A., Lera, F., Villarroel, J.L., 2010. Accurately locating a vertical magnetic dipole buried in a conducting earth. IEEE Trans. Geosci. Remote Sens. 48 (10), 3676–3685.

Brugger, H., Durrer, B., Adler-Kastner, L., Falk, M., Tschirky, F., 2001. Field management of avalanche victims. Resuscitation 51 (1), 7–15.

Brugger, H., Durrer, B., Elsesohn, F., Paal, P., Strapazzon, G., Winterberger, E., Zafren, K., Boyd, J., 2013. Resuscitation of avalanche victims: evidence-based guidelines of the international commission for mountain emergency medicine (ICAR MEDCOM): intended for physicians and other advanced life support personnel. Resuscitation 84 (5), 539–546.

Calvo, C., Villarroel, J.L., Cuchí, J.A., 2005. Valores de conductividad eléctrica de nieve y suelo a lo largo de un transecto longitudinal en el Pirineo. Rev. Cienc. Lucas Mallada 12, 101–112.

CISA-ICAR, 2010. People rescued from snow avalanches — alive or dead. URL http://www.ikar-cisa.org/.

Colbeck, S., 1982. The geometry and permittivity of snow at high-frequencies. J. Appl. Phys. 53 (6), 4495–4500.

Edgerly, B., 2002. Pinpointing on a line: a modern technique for solving deep burials. International Snow Science Workshop, ISSW. Penticton, British Columbia, 29 September–4 October 2002, pp. 463–466.

ETSI, 2001. Electromagnetic compatibility and radio spectrum matters (ERM); avalanche beacons; transmitter–receiver systems. ETSI EN 300 718–1. European standard (telecommunication series). European Telecommunications Standards Institute.

Etter, H.J., Meister, R., Atkins, D., 2004. ICAR and its importance in avalanche rescue. International Snow Science Workshop, ISSW. Jackson Hole, WY, 19–24 September 2004, pp. 360–369.

Falk, M., Brugger, M., Adler-Kastner, L., 1994. Avalanche survival chances. Nature 368 (1), 21.

Frolov, A.D., Macheret, Y.Y., 1999. On dielectric properties of dry and wet snow. Hydrol. Process. (13), 1755–1760.

Genswein, M., Reiweger, I., Schweizer, J., 2009. Survival chance optimized search strip width in avalanche rescue. Cold Reg. Sci. Technol. 59 (2–3), 259–266.

Haegeli, P., Falk, M., Brugger, H., Etter, H.-J., Boyd, J., 2011. Comparison of avalanche survival patterns in Canada and Switzerland. Can. Med. Assoc. J. 183 (7), 789–795.

Hellberg, F., Exner, T., Steinmüller, S., Stelzer, C., 2014. Avalanche transceiver test 2013–14. Tech. rep. Safety Research Group of the German Alpine Club (DAV) (URL http://www.alpenverein.de/chameleon/public/1f395617-d153-e5c6-a9e5-6ef7f56e800a/1-avalanche-transceiver-test-2013_2014_23569.pdf).

Herique, A., Kofman, W., 1997. Determination of the ice dielectric permittivity using the data of the test in Antarctica of the ground-penetration radar for Mars'98 mission. IEEE Trans. Geosci. Remote Sens. 35 (5), 1338–1349.

Jomelli, J., Delval, C., Grancher, D., Escande, S., Brunstein, D., Hetu, B., Filion, L., Pech, P., 2007. Probabilistic analysis of recent snow avalanche activity and weather in the French Alps. Cold Reg. Sci. Technol. (1–2), 180–192.

Keller, G.V., 1966. Electrical properties of rocks and minerals. In: Clark, S.P. (Ed.), Handbook of physical constants. The Geological Society of America, Inc., New York.

Lind, D.A., 1994. Understanding the avalanche beacon for best performance. International Snow Science Workshop, ISSW. Snowbird, Utah, 30 October-3 November, pp. 415–422.

Lind, D.A., Smythe, W., 1984. Avalanche beacons-working principles, specifications and comparative properties. International Snow Science Workshop, ISSW. Aspen, Colorado, 24–27 November 1984, pp. 48–53.

Matzner, R., 2008. A systematic approach to optimize avalanche beacon design for minimum search time. International Snow Science Workshop, ISSW. Whistler, BC, Canada, 21–27 September 2008, pp. 45–51.

Meier, F., 2006. On the effects of receiver bandwidth on the performance of avalanche beacons. International Snow Science Workshop, ISSW. Telluride, Colorado, USA, 1–6 October 2006.

Michahelles, F., Matter, P., Schmidt, A., Schiele, B., 2003. Applyng wearable sensors to avalanche rescue. Comput. Graph. 27 (6), 839–847.

Orellana, E., 1982. Prospección geoeléctrica en corriente contínua. Biblioteca técnica Philips, Paraninfo, Madrid.

Piniés, P., Tardós, J.D., 2006. Fast localization of avalanche victims using Sum of Gaussians. IEEE International Conference on Robotics and Automotion. Orlando, Florida, USA, pp. 3989–3994.

Salós, C.D., Lera, F., Villarroel, J.L., 2007. Digital signal processing in triple antenna arvas. IEEE International Conference on Signal Processing and Communication. Dubai, UAE, pp. 484–487.

Schreilechner, M., Eck, M., Schober, M., 2010. Simple and reliable methodology to compare various avalanche beacons taking into account the useful range, multiple burial, and the strength of the third antenna. International Snow Science Workshop, ISSW. Lake Tahoe, USA, 17–22 October 2010.

Schweizer, J., 2007. Determining the search width based on range measurements. URL. http://avalancheinfo.net/Newsletters%20and%20Articles/Articles/Search%20strip%20width%20Jurg%20Schweizer%202007.pdf.

Schweizer, J., Krüsi, G., 2003. Testing the performance of avalanche transceivers. Cold Reg. Sci. Technol. 37 (3), 429–438.

Siegel, M., King, R.W., 1970. Electromagnetic fields in a dissipative half-space: a numerical approach. J. Appl. Phys. 41 (6), 2415–2423.

Slotta-Bachmayr, L., 2005. How burial time of avalanche victims is influenced by rescue method: an analysis of search reports from the alps. Nat. Hazards 34, 341–352.

Sommerfeld, A., 1909. Über die Ausbreitung der Wellen in der drahtlosen Telegraphie. Ann. Phys. 28, 665–737.

Sommerfeld, A., 1926. Über die Ausbreitung der Wellen in der drahtlosen Telegraphie. Ann. Phys. 81, 1135–1153.

Tschirky, F., Brabec, B., Kern, M., 2000. Avalanche rescue systems in Switzerland: experience and limitations. International Snow Science Workshop, ISSW. Big Sky MT, USA, 2–6 October 2000, pp. 369–376.

Valt, M., Chiambretti, I., Zasso, R., 2009. 1985–2009 twenty-five years of avalanche accidents in Italy. International Snow Science Workshop, ISSW. Davos, Switzerland, 27 September–2 October 2009, pp. 686–690.

Wait, J.R., 1961. The electromagnetic fields of a horizontal dipole in the presence of a conducting half-space. Can. J. Phys. 39, 1017–1028.

Wait, J.R., 1969. Electromagnetic fields of sources in lossy media. Antenna Theory, Part 2. McGraw-Hill, pp. 438–556 (Ch. 24).

Wait, J.R., 1972. Locating an oscillating magnetic dipole in the earth. Electron. Lett. 8 (16), 404–406.

Wait, J.R., 1982. Geo-Electromagnetism. Academic Press, London.

Wait, J.R., 1996. Electromagnetic Waves in Stratified Media. IEEE/OUP series on electromagnetic wave theory. IEEE Press in assoc. with Oxford University Press.

Zweifel, B., Techel, F., Björk, C., 2012. Who is involved in avalanche accidents? International Snow Science and Workshop, ISSW. Anchorage, Alaska, 16–21 September 2012, pp. 234–239.